STRESS–DILATANCY BASED MODELLING OF GRANULAR MATERIALS AND EXTENSIONS TO SOILS WITH CRUSHABLE GRAINS

Antonio DeSimone*
Claudio Tamagnini[†]

Trieste, 20/10/2004

Abstract

Stress–dilatancy relations have played a crucial role in the understanding of the mechanical behavior of soils and in the development of realistic constitutive models for their response. Recent investigations on the mechanical behavior of materials with crushable grains have called into question the validity of classical relations such as those used in Critical State Soil Mechanics.

In this paper, a method to construct thermodynamically consistent (isotropic, three–invariant) elasto–plastic models based on a given stress–dilatancy relation is discussed. Extensions to cover the case of granular materials with crushable grains are also presented, based on the interpretation of some classical model parameters (e.g., the stress ratio at critical state) as internal variables that evolve according to suitable hardening laws.

*SISSA – International School for Advanced Studies, Trieste, Italy, desimone@sissa.it
[†]Università degli Studi di Perugia, via G. Duranti, 93, 06125 Perugia, Italy, tamag@unipg.it

Contents

1   Introduction

In recent years, granular materials whose mechanical response is affected by changes of internal micro–structure induced by the loading process have attracted considerable attention, from the point of view of both theory and experiment. These include, in particular, materials with crushable grains [24], [30], [14], [39], weak rocks or cemented aggregates whose bonds suffer progressive degradation due to applied loads and other physico–chemical mechanisms [33, 3, 1], [42, 17, 31, 43], and structured clays [15, 50].

In view of the expected strong non–linearities, a detailed understanding of the behavior of such materials seems necessary for reliable quantitative predictions of their mechanical response in engineering applications, such as: i) stability of natural slopes and open cuts , see e.g. [9]; ii) tunnelling and underground excavations, see e.g. [7]; iii) driven piles in calcareous soils, see e.g. [2, 16, 6]. In addition, research on these materials offers an opportunity to assess critically and to reconsider some of the central hypotheses underlying continuum theories developed for soils and, in particular, Critical State Soil Mechanics (CSSM). The key question to be addressed is: how do grain crushing and debonding affect the macroscopic properties of a granular aggregate? From the point of view of CSSM, this amounts to asking how the evolution of the micro–structure affects yield surfaces, flow rules and hardening laws. There are many complementary angles of attack to this question. One of them, explored, e.g., in [35], is to try and deduce macroscopic constitutive equations from micromechanical consideration of some underlying microscopic process. Another, more macroscopic possibility is to probe experimentally the limits of applicability of existing theories, to single out those macroscopic parameters which are sensitive to changes of microstructure, and to identify the new ingredients that are needed to capture the macroscopic fingerprints of the microscopic processes. The experimental background of our present study [10], together with [8], give an example of this second approach.

An extensive experimental campaign on Pozzolana Nera (PN), a weak pyroclastic rock from the region South–East of Rome, has revealed a number of peculiar features in the mechanical properties of this material that may be attributed to the changes of the internal structure induced by loading [10]. PN is an extremely polydisperse granular material, as shown in Figure 1. Bonds and grains are made of the same constituents, so that grain crushing and bond breaking are two complementary aspects of the same destructuration phenomenon. The material does crush at rather small loads, as shown in Figure 2. This results in observed stress–dilatancy curves which are at odds with one of the most basic ingredients of CSSM models, namely, the existence of a well defined one–to–one relation between dilatancy and stress ratio at yield [56].

To place this discussion into context, let us recall that a stress–dilatancy relation is an identity of the type

$$\eta_y := \frac{q_y}{p_y} = \Phi(d) \tag{1.1}$$

linking the ratio η of deviatoric to volumetric components of the stress at yield and the dilatancy $d := \dot{\epsilon}_v^p / \dot{\epsilon}_s^p$, i.e., the ratio between volumetric and deviatoric components of the plastic deformation rate. Relationships of this kind have played a fundamental role in understanding and interpreting the observed

3
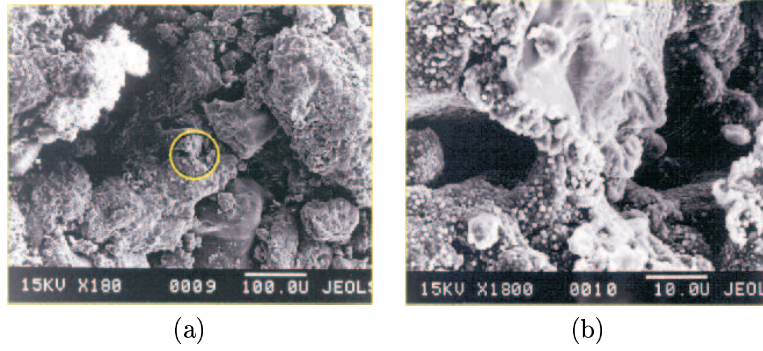
Figure 1: Scanning electron micrographs of Pozzolana Nera at increasing magnification factors (adapted from [10]). a) magnification 180×; b) blow–up of circled area in (a), at 1800×.
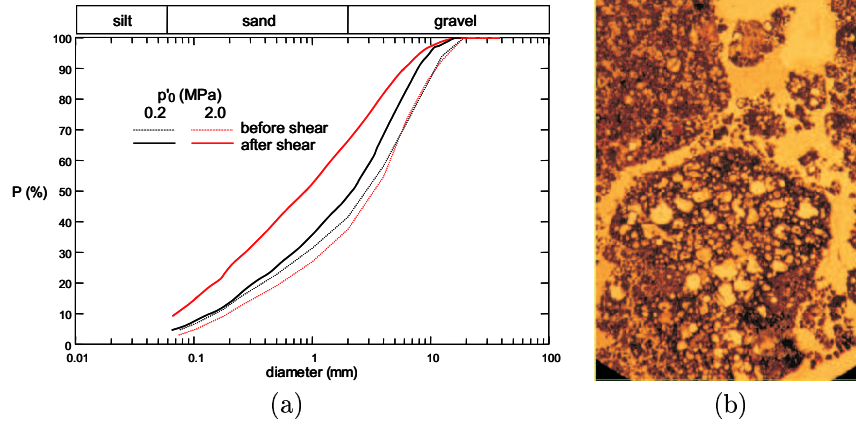

Figure 2: Quantitative and visual evidence of grain crushing in Pozzolana Nera. a) grading curves before and after TX compression tests at increasing confining stress (after [10]); b) thin section of grains crushed after shear (adapted from [11]).

4

behavior of granular materials, see e.g. [48, 49, 51, 52], as well as in the formulation of constitutive models within CSSM. In particular, setting $\Phi(d) = M - d$ in (1.1), one obtains

$$\frac{q_y}{p_y} = M - d \tag{1.2}$$

defining the original Cam–Clay model, see, e.g., [53].

In hindsight, that a relation like (1.1) should fail in a material with crushable grains is not too surprising. Equation (1.2) expresses the fundamental fact that, in order to shear a dilatant material ($d < 0$), one has to apply extra shear stress to overcome the work that pressure expends against the increase of volume. Dilation is due to rearrangements of the internal micro–structure, with increase of void ratio for an initially dense material, and decrease for an initially loose specimen. No material can dilate forever: the hardening laws of Cam Clay are such that an asymptotic state (the critical state, defined by the condition $d = 0$) is always reached under monotonic shearing. At critical state, the void ratio has reached a characteristic steady value, and the frictional behavior of the granular assembly (in particular, the stress ratio at critical state, M) depends only on the intrinsic properties of the solid skeleton (say, the size distribution, the shape, and the angularity of the grains), and not on its initial relative density.

The argument above shows, however, that if a material has crushable grains, then parameter M should be thought of as a quantity able to evolve with the changes of grading induced by the loading process. This is the key idea behind a constitutive model proposed in [8] to explain the observed stress–dilatancy curves in PN. Let us assume, for the sake of the argument, the existence of a virgin state for the intact material and of a fully degraded state for the material which has undergone grain crushing and debonding. At each instant of a loading process starting from the virgin sate, the current state of the material is intermediate between the virgin and the fully degraded state, and it may be described through the use of internal variables which evolve during the loading process. In particular, parameter M evolves, typically decreasing as the grains crush. Each intermediate state is characterized by a one–to–one (e.g., linear as in (1.2)) relationship between d and η_y while the d:η_y paths traced upon loading result from the material spanning with continuity different intermediate states. This may give rise to stress–dilatancy relations which are not one–to–one, as observed in PN, see Figure 3.

The goal of this paper is to place the model proposed in [8] on a thermodynamically sound basis. We do this in two steps. First, we focus on the thermodynamic structure of models of soil behavior which are consistent with a given (one–to–one) stress–dilatancy relation. This will lead to the proposal of a general method to construct (three–invariant, isotropic) models which stem from such relations. Later, we extend the range of validity of this approach to deal with the case of crushable grains, for which more complex stress–dilatancy relation are to be expected.

Given the complexity of the phenomena involved at the microscopic level, it seems advisable to ensure thermodynamic consistency at the macroscopic level, by relying as much as possible on a thermodynamically consistent formulation of flow rules and hardening laws. Moreover, rather than being interested in fitting specific sets of data, we are after sharp predictions of qualitative features and trends which can be used as conceptual benchmarks. For these reasons, we
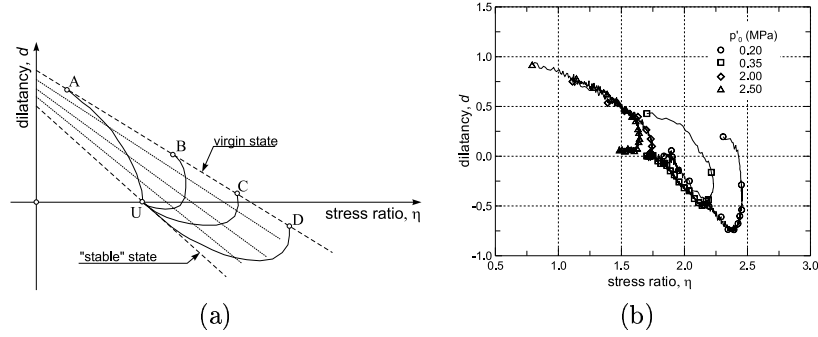
Figure 3: Stress–dilatancy relation for a material with crushable grains. a) conceptual sketch; b) experimental evidence for Pozzolana Nera (after [10]).

place ourselves in the tighter environment of associative models, with respect to both flow rules and hardening laws. Non–associativity can easily be brought back if so required by experimental evidence, as in [8].

The paper is organized as follows. We review the essentials of rate-independent elasto–plasticity in Section 2, mostly to fix notation. In Section 3 we specialize to the associative case, discussing two dual formulations: direct (i.e., based on yield surfaces and flow rules) and dual (i.e., based on a dissipation potential). The two formulations are summarized in Boxes 1 and 2. Their equivalence, given by equation (3.19), is the main result of this section. The flexibility gained by moving back and forth between direct and dual formulation is used in Section 4 to propose a method to construct three-invariant isotropic models consistent with a given stress–dilatancy relation. The method is summarized in Box 3. Given the relevance of stress–dilatancy relations for the subject matter of this paper, their conceptual status with respect to direct and dual flow rules is reviewed in subsection 4.5. Finally, in Section 5, a specific choice of yield function is made, and hardening laws are proposed to describe the impact of debonding and grain crushing on the predicted macroscopic response.

Throughout the paper, the stress tensor and all the related quantities are effective stresses as defined by Terzaghi, unless otherwise stated. The usual sign convention of soil mechanics (compression positive) is adopted throughout. Direct notation is used to represent vector and tensor quantities. Following standard notation, for any two vectors $v, w \in \mathbb{R}^3$, the dot product is defined as: $v \cdot w := v_i w_i$, and the dyadic product as: $[v \otimes w]_{ij} := v_i w_j$. Similarly, for any two second–order tensors x, y, $x \cdot y := x_{ij} y_{ij}$ and $[x \otimes y]_{ijkl} := x_{ij} y_{kl}$.

2 Flow theory of rate–independent elasto–plasticity

We start with the additive decomposition of strain

$$\epsilon = -\frac{1}{2}(\nabla u + \nabla u^T) \tag{2.1}$$

6

where u is the displacement, into elastic, reversible part $\boldsymbol{\epsilon}^e$ and plastic, irreversible part $\boldsymbol{\epsilon}^p$:

$$\boldsymbol{\epsilon} = \boldsymbol{\epsilon}^e + \boldsymbol{\epsilon}^p\,. \tag{2.2}$$

In addition, we introduce an array of strain-like internal variables $\boldsymbol{\xi}$ describing changes of the microstructure of the material (associated with, say, hardening, debonding, grain crushing , etc.), and define a generalized plastic strain

$$\boldsymbol{\alpha} = (\boldsymbol{\epsilon}^p, \boldsymbol{\xi}) \tag{2.3}$$

For the free energy density $\psi = \psi(\boldsymbol{\epsilon}^e, \boldsymbol{\xi})$, assuming that elastic moduli are not affected by microstructure changes, the following additive decomposition holds

$$\psi(\boldsymbol{\epsilon}^e, \boldsymbol{\xi}) = \psi^e(\boldsymbol{\epsilon}^e) + \psi^p(\boldsymbol{\xi})\,. \tag{2.4}$$

The stress-like variables, work-conjugate to $\boldsymbol{\epsilon}$ and $\boldsymbol{\xi}$ are thus

$$\boldsymbol{\sigma}(\boldsymbol{\epsilon}^e) = \frac{\partial \psi^e}{\partial \boldsymbol{\epsilon}^e} \qquad\qquad \boldsymbol{\chi}(\boldsymbol{\xi}) = -\frac{\partial \psi^p}{\partial \boldsymbol{\xi}} \tag{2.5}$$

and they define a generalized stress A

$$\boldsymbol{A} = (\boldsymbol{\sigma}, \boldsymbol{\chi})\,. \tag{2.6}$$

We assume that $(2.5)_2$ is invertible and write

$$\boldsymbol{\xi} = \hat{\boldsymbol{\xi}}(\boldsymbol{\chi}) \tag{2.7}$$

for the inverse. The dissipation inequality reads

$$\boldsymbol{\sigma} \cdot \dot{\boldsymbol{\epsilon}} - \dot{\psi} = \boldsymbol{\sigma} \cdot \dot{\boldsymbol{\epsilon}}^p + \boldsymbol{\chi} \cdot \dot{\boldsymbol{\xi}} =: \mathcal{D} \geqslant 0 \tag{2.8}$$

where $\mathcal{D}$, the dissipation (in fact, the volumetric density of the rate of dissipation), can also be written as

$$\mathcal{D} = \boldsymbol{A} \cdot \dot{\boldsymbol{\alpha}}\,. \tag{2.9}$$

The yield function is

$$f(\boldsymbol{\sigma}, \boldsymbol{\chi}; \boldsymbol{\zeta}) = F(\boldsymbol{A}; \boldsymbol{\zeta}) \leq 0 \tag{2.10}$$

where $\boldsymbol{\zeta}$ are hardening parameters which, contrary to those contained in $\boldsymbol{\chi}$, have no corresponding work-conjugate strain-like variables. The evolution laws for $\boldsymbol{\epsilon}^p$ and $\boldsymbol{\xi}$ are the flow rules

$$\dot{\boldsymbol{\epsilon}}^p = \dot{\gamma}\,\boldsymbol{r}\,(\boldsymbol{\sigma}, \boldsymbol{\chi}; \boldsymbol{\zeta}) \tag{2.11}$$

$$\dot{\boldsymbol{\xi}} = \dot{\gamma}\,\boldsymbol{h}\,(\boldsymbol{\sigma}, \boldsymbol{\chi}; \boldsymbol{\zeta})\,. \tag{2.12}$$

Note that the plastic flow direction tensor $\boldsymbol{r}$ is typically defined in terms of the gradient of a scalar function g, known as plastic potential, so that eq. (2.11) is often written as:

$$\dot{\boldsymbol{\epsilon}}^p = \dot{\gamma}\frac{\partial g}{\partial \boldsymbol{\sigma}}(\boldsymbol{\sigma}, \boldsymbol{\chi}; \boldsymbol{\zeta})\,. \tag{2.13}$$

The evolution laws for the hardening parameters $\boldsymbol{\zeta}$ are called hardening laws

$$\dot{\boldsymbol{\zeta}} = -\dot{\gamma}\, \boldsymbol{z}(\boldsymbol{\sigma}, \boldsymbol{\chi}; \boldsymbol{\zeta}) \tag{2.14}$$

Note that the flow rule for $\boldsymbol{\xi}$ induces an evolution law for $\boldsymbol{\chi}$. This is also a hardening law which takes, however, the special form

$$\dot{\boldsymbol{\chi}} = -\frac{\partial^2 \psi^p(\boldsymbol{\xi})}{\partial \boldsymbol{\xi} \otimes \partial \boldsymbol{\xi}} \, \dot{\boldsymbol{\xi}} = -\dot{\gamma}\, \frac{\partial^2 \psi^p(\boldsymbol{\xi})}{\partial \boldsymbol{\xi} \otimes \partial \boldsymbol{\xi}} \, \boldsymbol{h}\,. \tag{2.15}$$

Defining the symmetric tensors of hardening moduli

$$\mathbb{D}_\xi(\boldsymbol{\xi}) := \frac{\partial^2 \psi^p}{\partial \boldsymbol{\xi} \otimes \partial \boldsymbol{\xi}} \qquad\qquad \mathbb{D}_\chi(\boldsymbol{\chi}) := \mathbb{D}_\xi(\hat{\boldsymbol{\xi}}(\boldsymbol{\chi})) \tag{2.16}$$

and the tensor of elastic moduli

$$\mathbb{D}^e = \frac{\partial^2 \psi^e}{\partial \boldsymbol{\epsilon}^e \otimes \partial \boldsymbol{\epsilon}^e} \tag{2.17}$$

we get the relations

$$\dot{\boldsymbol{\sigma}} = \mathbb{D}^e(\dot{\boldsymbol{\epsilon}} - \dot{\boldsymbol{\epsilon}}^p) \tag{2.18}$$

$$\dot{\boldsymbol{\chi}} = -\dot{\gamma}\mathbb{D}_\chi\, \boldsymbol{h}\,. \tag{2.19}$$

Plastic flow is governed by the Karush–Kuhn–Tucker (KKT) conditions

$$\dot{\gamma} \geqslant 0 \quad,\quad \dot{\gamma} f = 0 \tag{2.20}$$

(recall that, by definition, $f \leq 0$), implying that plastic flow ($\dot{\gamma} > 0$) can occur only at yield ($f = 0$). In a time interval in which it does not vanish, the plastic multiplier $\dot{\gamma}$ is obtained from the consistency condition $f \equiv 0$, leading to

$$\dot{f} \leq 0, \quad \dot{\gamma}\dot{f} = 0 \tag{2.21}$$

so that

$$\dot{\gamma} > 0 \quad \Rightarrow \quad \dot{f} = \frac{\partial f}{\partial \boldsymbol{\sigma}} \cdot \dot{\boldsymbol{\sigma}} + \frac{\partial f}{\partial \boldsymbol{\chi}} \cdot \dot{\boldsymbol{\chi}} + \frac{\partial f}{\partial \boldsymbol{\zeta}} \cdot \dot{\boldsymbol{\zeta}} = 0\,. \tag{2.22}$$

Using the expressions (2.14), (2.18), (2.19) for $\dot{\boldsymbol{\zeta}}$, $\dot{\boldsymbol{\sigma}}$, $\dot{\boldsymbol{\chi}}$, and in view of the flow rule (2.11), (2.22) implies

$$\dot{\gamma} = \frac{1}{K_p}\left(\frac{\partial f}{\partial \boldsymbol{\sigma}} \cdot \mathbb{D}^e\, \dot{\boldsymbol{\epsilon}}\right) \tag{2.23}$$

whenever $\dot{\gamma}$ does not vanish, where the plastic modulus

$$K_p = \frac{\partial f}{\partial \boldsymbol{\sigma}} \cdot \mathbb{D}^e\, \boldsymbol{r} + \frac{\partial f}{\partial \boldsymbol{\chi}} \cdot \mathbb{D}_\chi\, \boldsymbol{h} + \frac{\partial f}{\partial \boldsymbol{\zeta}} \cdot \boldsymbol{z} \tag{2.24}$$

is assumed to be strictly positive. Plugging (2.23) into (2.11) and substituting in (2.18) we get

$$\dot{\boldsymbol{\sigma}} = \begin{cases} \mathbb{D}^e\, \dot{\boldsymbol{\epsilon}} & \text{if } \dot{\gamma} = 0 \\ \mathbb{D}^{ep}\, \dot{\boldsymbol{\epsilon}} & \text{if } \dot{\gamma} > 0 \end{cases} \tag{2.25}$$

where

$$\mathbb{D}^{ep} = \mathbb{D}^e - \frac{1}{K_p}\left(\mathbb{D}^e\, \boldsymbol{r} \otimes \mathbb{D}^e\, \frac{\partial f}{\partial \boldsymbol{\sigma}}\right)\,. \tag{2.26}$$

3   Associative plasticity: yield function and dissipation potential

The flow rules are said to be associative if

$$r\,(\boldsymbol{\sigma},\boldsymbol{\chi};\boldsymbol{\zeta}) = \frac{\partial}{\partial\boldsymbol{\sigma}}f(\boldsymbol{\sigma},\boldsymbol{\chi};\boldsymbol{\zeta}) \tag{3.1}$$

$$h\,(\boldsymbol{\sigma},\boldsymbol{\chi};\boldsymbol{\zeta}) = \frac{\partial}{\partial\boldsymbol{\chi}}f(\boldsymbol{\sigma},\boldsymbol{\chi};\boldsymbol{\zeta}) \tag{3.2}$$

so that

$$\dot{\boldsymbol{\epsilon}}^p = \dot{\gamma}\,\frac{\partial f}{\partial\boldsymbol{\sigma}} \tag{3.3}$$

$$\dot{\boldsymbol{\xi}} = \dot{\gamma}\,\frac{\partial f}{\partial\boldsymbol{\chi}} \tag{3.4}$$

or, in a more compact form

$$\dot{\boldsymbol{\alpha}} = \dot{\gamma}\,\frac{\partial F}{\partial\boldsymbol{A}}\,. \tag{3.5}$$

The hardening law for $\boldsymbol{\chi}$ becomes

$$\dot{\boldsymbol{\chi}} = -\dot{\gamma}\,\mathbb{D}_\chi\,(\boldsymbol{\chi})\frac{\partial f}{\partial\boldsymbol{\chi}} \tag{3.6}$$

By analogy, the hardening law for $\boldsymbol{\zeta}$ is said to be associative if it can be expressed in the form

$$\dot{\boldsymbol{\zeta}} = -\dot{\gamma}\,\mathbb{D}_\zeta\,(\boldsymbol{\zeta})\frac{\partial f}{\partial\boldsymbol{\zeta}} \qquad\qquad \boldsymbol{z} := \mathbb{D}_\zeta\,(\boldsymbol{\zeta})\frac{\partial f}{\partial\boldsymbol{\zeta}}\,. \tag{3.7}$$

The plastic modulus takes now the expression

$$K_p = \mathbb{D}^e\,\frac{\partial f}{\partial\boldsymbol{\sigma}}\cdot\frac{\partial f}{\partial\boldsymbol{\sigma}} + \mathbb{D}_\chi\,\frac{\partial f}{\partial\boldsymbol{\chi}}\cdot\frac{\partial f}{\partial\boldsymbol{\chi}} + \mathbb{D}_\zeta\,\frac{\partial f}{\partial\boldsymbol{\zeta}}\cdot\frac{\partial f}{\partial\boldsymbol{\zeta}} \tag{3.8}$$

while formula (2.23) for the plastic multiplier $\dot{\gamma}$ is unchanged. Note that, in the associative case, K_p is certainly positive, provided that the tensors of elastic and hardening moduli $\mathbb{D}^e$, $\mathbb{D}_\chi$, and $\mathbb{D}_\zeta$ are positive definite. Positivity of $\mathbb{D}^e$ and $\mathbb{D}_\chi$ is guaranteed if ψ^e and ψ^p are strictly convex.

The tensor of tangent (elasto-plastic) moduli is given by

$$\mathbb{D}^{ep} = \mathbb{D}^e - \frac{1}{K_p}\,(\mathbb{D}^e\,\frac{\partial f}{\partial\boldsymbol{\sigma}}\otimes\mathbb{D}^e\,\frac{\partial f}{\partial\boldsymbol{\sigma}}) \tag{3.9}$$

showing that, whenever the flow rule for $\boldsymbol{\epsilon}^p$ is associative, $\mathbb{D}^{ep}$ is symmetric. If, in addition, also the hardening laws are associative, the symmetry property is carried over to the algorithmic moduli consistent with the Backward Euler closest–point projection algorithms widely used in computational plasticity, see [54].

Associativity confers to the flow theory of rate–independent elasto–plasticity a very rich structure through the use of convex duality. Rather than using a

formulation based on a yield function in stress space which delivers flow rules for the conjugate strain–like variables, one may start from a dissipation function $\mathcal{D}$ depending on the rates of strain–like quantities, and derive the conjugate stress–like variables through differentiation. Thermodynamic consistency is thus guaranteed by the properties of $\mathcal{D}$. This is a key achievement of the French School, [38, 18, 22, 19], see also [34, 45, 23]. The same format has been first used in Soil Mechanics in [37]. The advantages of ensuring thermodynamic consistency in the constitutive modelling of soils has been emphasized by Houlsby [26, 27] and implemented in a number of concrete models of soil behavior, see e.g. [13, 28, 12]

To illustrate the use of convex duality, let us start from the yield function F of (2.10) in which we drop, for simplicity, the dependence on $\boldsymbol{\zeta}$, and let us denote by $\mathcal{A}$ the set of admissible $\dot{\boldsymbol{\alpha}}$ and by $\mathcal{A}^*$ the set of admissible $\boldsymbol{A}$. Assume that the yield locus

$$\mathcal{K} = \{\boldsymbol{A} \in \mathcal{A}^* : F(\boldsymbol{A}) \leq 0\} \tag{3.10}$$

defined by F is a closed convex set containing the origin, and define the indicator function of $\mathcal{K}$ as

$$I_{\mathcal{K}}(\boldsymbol{A}) = \begin{cases} 0 & \text{if } \boldsymbol{A} \in \mathcal{K} \\ +\infty & \text{otherwise.} \end{cases} \tag{3.11}$$

The flow rule (3.5) can be written as

$$\dot{\boldsymbol{\alpha}} \in \partial I_{\mathcal{K}}(\boldsymbol{A}) = N_{\mathcal{K}}(\boldsymbol{A}) \tag{3.12}$$

where $\partial I_{\mathcal{K}}(\boldsymbol{A})$ is the subgradient of $I_{\mathcal{K}}$ at $\boldsymbol{A}$ and $N_{\mathcal{K}}(\boldsymbol{A})$ is the normal cone to $\mathcal{K}$ at $\boldsymbol{A}$, see e.g. [46, 23, 5]. The identity in (3.12) is a classical result of convex analysis. Note that, if $\boldsymbol{A}$ is on the boundary of $\mathcal{K}$, then (3.12) expresses normality of $\dot{\boldsymbol{\alpha}}$ to $\partial \mathcal{K}$, while if $\boldsymbol{A}$ is in the interior of $\mathcal{K}$, then (3.12) implies that $\dot{\boldsymbol{\alpha}} = 0$. Consider now the Legendre–Fenchel transform of $I_{\mathcal{K}}$

$$(I_{\mathcal{K}})^*(\dot{\boldsymbol{\alpha}}) = \sup_{\boldsymbol{A} \in \mathcal{A}^*} \{\boldsymbol{A} \cdot \dot{\boldsymbol{\alpha}} - I_{\mathcal{K}}(\boldsymbol{A})\} = \sup_{\boldsymbol{A} \in \mathcal{K}} \boldsymbol{A} \cdot \dot{\boldsymbol{\alpha}}. \tag{3.13}$$

It is easy to show[1] that, in fact, $(I_{\mathcal{K}})^*$ is the dissipation function

$$(I_{\mathcal{K}})^*(\dot{\boldsymbol{\alpha}}) = \mathcal{D}(\dot{\boldsymbol{\alpha}}). \tag{3.14}$$

A fundamental result of convex analysis[2], relating the subgradients of a function and of its Legendre transform, then implies that

$$\dot{\boldsymbol{\alpha}} \in N_{\mathcal{K}}(\boldsymbol{A}) \Leftrightarrow \boldsymbol{A} \in \partial \mathcal{D}(\dot{\boldsymbol{\alpha}}). \tag{3.15}$$

This shows that the associative flow rule $\dot{\boldsymbol{\alpha}} \in N_{\mathcal{K}}(\boldsymbol{A})$ for $\boldsymbol{\alpha}$ leads to the prescription $\boldsymbol{A} \in \partial \mathcal{D}(\dot{\boldsymbol{\alpha}})$ for the conjugate stress variable $\boldsymbol{A}$.

---

[1]Indeed, if $\dot{\boldsymbol{\alpha}} = 0$, then both $(I_{\mathcal{K}})^*(\dot{\boldsymbol{\alpha}})$ and $\mathcal{D}(\dot{\boldsymbol{\alpha}})$ vanish. If instead $\dot{\boldsymbol{\alpha}} \neq 0$, then by normality

$$\bar{\boldsymbol{A}} := \arg\max_{\boldsymbol{A} \in \mathcal{K}} \boldsymbol{A} \cdot \dot{\boldsymbol{\alpha}}$$

is such that $\dot{\boldsymbol{\alpha}} \in N_{\mathcal{K}}(\bar{\boldsymbol{A}})$ and both $(I_{\mathcal{K}})^*(\dot{\boldsymbol{\alpha}})$ and $\mathcal{D}(\dot{\boldsymbol{\alpha}})$ equal $\bar{\boldsymbol{A}} \cdot \dot{\boldsymbol{\alpha}}$. The physical interpretation of this result, obtained by comparing eqs. (3.13) and (3.14), is that associative plastic flow obeys the principle of maximum dissipation.

[2]We are using convex duality, i.e., the fact that if f^* is the Legendre transform of a convex function f, and if ∂f^* and ∂f are their subgradients, then

$$x^* \in \partial f(x) \Leftrightarrow x \in \partial f^*(x^*)$$

see, e.g., [46].

Box 1. From yield-locus-based to dissipation-based formulation.

F	yield function
$\mathcal{K} = \{\boldsymbol{A} : F(\boldsymbol{A}) \leq 0\}$	elastic domain and yield locus (a closed convex set containing the origin)
$I_{\mathcal{K}}(\boldsymbol{A}) = \begin{cases} 0 & \text{if } \boldsymbol{A} \in \mathcal{K} \\ +\infty & \text{otherwise} \end{cases}$	indicator function of $\mathcal{K}$
$(I_{\mathcal{K}})^*(\dot{\boldsymbol{\alpha}}) = \sup_{\boldsymbol{A} \in \mathcal{K}} \boldsymbol{A} \cdot \dot{\boldsymbol{\alpha}}$	Legendre–Fenchel transform of $I_{\mathcal{K}}$
$\mathcal{D}(\dot{\boldsymbol{\alpha}}) = (I_{\mathcal{K}})^*(\dot{\boldsymbol{\alpha}})$	dissipation function
$\partial \mathcal{D}^*(\boldsymbol{A}) = \partial I_{\mathcal{K}}(\boldsymbol{A}) = N_{\mathcal{K}}(\boldsymbol{A})$	from convex analysis ($N_{\mathcal{K}}(\boldsymbol{A})$ normal cone to $\mathcal{K}$ at $\boldsymbol{A}$)
$\dot{\boldsymbol{\alpha}} \in N_{\mathcal{K}}(\boldsymbol{A}) \Rightarrow \boldsymbol{A} \in \partial \mathcal{D}(\dot{\boldsymbol{\alpha}})$	from convex duality

To illustrate the reverse path, let $\mathcal{D}$ be a given dissipation function. We assume that $\mathcal{D}(\dot{\boldsymbol{\alpha}})$ is a gauge, i.e., a non–negative, convex, lower–semi–continuous, positively homogeneous function of degree one vanishing at the origin. Define the set

$$\mathcal{K} = \{\boldsymbol{A} \in \mathcal{A}^* : \boldsymbol{A} \cdot \dot{\boldsymbol{\alpha}} \leq \mathcal{D}(\dot{\boldsymbol{\alpha}})\} \tag{3.16}$$

which is a closed, convex subset of $\mathcal{A}^*$ containing the origin. Note that on $\partial \mathcal{K}$, $\boldsymbol{A} \cdot \dot{\boldsymbol{\alpha}}$ matches $\mathcal{D}(\dot{\boldsymbol{\alpha}})$, hence $\boldsymbol{A}$ is a yield stress, while in the interior $\mathcal{K}^0$ of $\mathcal{K}$, $\boldsymbol{A} \cdot \dot{\boldsymbol{\alpha}} < \mathcal{D}(\dot{\boldsymbol{\alpha}})$ hence $\mathcal{K}^0$ is the elastic domain. $\mathcal{K}$ can be interpreted as the zero sublevel set of a yield function F by choosing any F such that $\{\boldsymbol{A} : F(\boldsymbol{A}) \leq 0\} \equiv \mathcal{K}$. For given $\mathcal{K}$, there is an arbitrariness in the selection of F which can be eliminated through a canonical choice, see [23]. We can now invoke a standard result of convex analysis which guarantees that the Legendre–Fenchel transform of a gauge is the indicator function of a closed convex set containing the origin. In fact, the Legendre transform of the dissipation function is the indicator function of $\mathcal{K}$

$$(\mathcal{D})^*(\boldsymbol{A}) = I_{\mathcal{K}}(\boldsymbol{A}) . \tag{3.17}$$

By convex duality, eq. (3.15), we can conclude that

$$\boldsymbol{A} \in \partial \mathcal{D}(\dot{\boldsymbol{\alpha}}) \Rightarrow \dot{\boldsymbol{\alpha}} \in N_{\mathcal{K}}(\boldsymbol{A}) , \tag{3.18}$$

i.e., if one prescribes an evolution process in which the stress–like quantities $\boldsymbol{A}$ are derived from the dissipation function $\mathcal{D}$, then the conjugate strain-like variables $\boldsymbol{\alpha}$ evolve according to the associative flow rule $\dot{\boldsymbol{\alpha}} \in N_{\mathcal{K}}(\boldsymbol{A})$.

The paths from classical (i.e., based on yield locus and normality rule) to dual (i.e., based on a dissipation potential) formulations of associative plasticity, and viceversa, are summarized in Boxes 1 and 2. For $\partial \mathcal{K}$ smooth, and if $\mathcal{D}$ is

Box 2. From dissipation-based to yield-locus-based formulation.

$\mathcal{D}$	dissipation function (a gauge)
$\mathcal{K} = \{\boldsymbol{A} : \boldsymbol{A} \cdot \dot{\boldsymbol{\alpha}} \le \mathcal{D}(\dot{\boldsymbol{\alpha}})\}$	elastic domain and yield locus (choose F such that $\{\boldsymbol{A} : F(\boldsymbol{A}) \le 0\} \equiv \mathcal{K}$)
$I_{\mathcal{K}}(\boldsymbol{A}) = (\mathcal{D})^*(\boldsymbol{A})$	Legendre–Fenchel transform of $\mathcal{D}$
$\partial\mathcal{D}^*(\boldsymbol{A}) = \partial I_{\mathcal{K}}(\boldsymbol{A}) = N_{\mathcal{K}}(\boldsymbol{A})$	from convex analysis
$\boldsymbol{A} \in \partial\mathcal{D}(\dot{\boldsymbol{\alpha}}) \Rightarrow \dot{\boldsymbol{\alpha}} \in N_{\mathcal{K}}(\boldsymbol{A})$	from convex duality

smooth away from $\dot{\boldsymbol{\alpha}} = 0$, we can rewrite (3.15) in the simpler form

$$\boldsymbol{A}_Y = \left.\frac{\partial}{\partial\dot{\boldsymbol{\alpha}}}\mathcal{D}(\dot{\boldsymbol{\alpha}})\right|_{\dot{\boldsymbol{\alpha}}\neq 0} \qquad \Leftrightarrow \qquad \dot{\boldsymbol{\alpha}} = \dot{\gamma}\left.\frac{\partial}{\partial\boldsymbol{A}}F(A)\right|_{A=A_Y} \qquad (3.19)$$

where $\boldsymbol{A}_Y$ is a yield value for $\boldsymbol{A}$, i.e., such that $F(\boldsymbol{A}_Y) = 0$. This is the key result of this section with respect to the further developments of this paper. The identity on the right side of the equivalence sign in (3.19) is the classical associative flow rule, according to which the generalized plastic strain rate is parallel to the gradient of the yield function F, hence normal to the yield surface $\{F = 0\}$. We will refer to the left side of (3.19) as the 'dual' (of the) flow rule.

4 Isotropic flow rules and yield criteria from a stress–dilatancy relation

The goal of this section is to show how specific forms of the flow rule and of the yield function can be inferred from experimental observations. Our primary experimental input comes from stress–dilatancy relations, which are commonly recorded in the experimental testing of geomaterials. Our method consists of deducing the yield locus from the combination of a stress–dilatancy relation with a dual flow rule, and it is applied to the derivation of a class of isotropic, three–invariant models.

4.1 Isotropy

We restrict our attention to isotropic models. Although this framework may prove too restrictive to capture such effect as stress–induced or inherent anisotropy, or to reproduce correctly the response to cyclic loading, it has the advantage to keep the mathematical structure of the model to an acceptable level of complexity. In many cases this may be the most reasonable compromise between the competing requirements of 'generality' and 'tractability' of the theory, in the spirit of, e.g., critical state models for fine–grained soils [53], [47], [56], or the works of Lade [29] and Nova [40, 44, 41] for coarse–grained soils. In fact, application of hardening elasto–plasticity to the numerical solution of practical

engineering problems remains, at present, mostly confined to isotropic models. The assumption of isotropy brings in the following consequences:

i) the strain–like and stress–like internal variables $\boldsymbol{\xi}$, $\boldsymbol{\chi}$, $\boldsymbol{\zeta}$ all consist of n-tuples of uncorrelated scalar quantites, i.e.,

$$\boldsymbol{\xi} = \{\xi_k\} \qquad (k = 1, \ldots, n_\xi) \qquad (4.1)$$

$$\boldsymbol{\chi} = \{\chi_k\} \qquad (k = 1, \ldots, n_\chi) \qquad (4.2)$$

$$\boldsymbol{\zeta} = \{\zeta_k\} \qquad (k = 1, \ldots, n_\zeta) \qquad (4.3)$$

ii) the dissipation function $\mathcal{D}$ depends on the plastic strain rate tensor $\dot{\boldsymbol{\epsilon}}^p$ only through its invariants, i.e.:

$$\mathcal{D}(\dot{\boldsymbol{\epsilon}}^p, \dot{\boldsymbol{\xi}}) = \tilde{\mathcal{D}}(\dot{\epsilon}_v^p, \dot{\epsilon}_s^p, z_\epsilon, \dot{\boldsymbol{\xi}}) \qquad (4.4)$$

where

$$\dot{\epsilon}_v^p = \mathrm{tr}(\dot{\boldsymbol{\epsilon}}^p), \quad \dot{\epsilon}_s^p = \left[\frac{2}{3}\mathrm{tr}(\dot{e}^{p2})\right]^{\frac{1}{2}}, \quad z_\epsilon = \sin(3\theta_\epsilon) = \sqrt{6}\frac{\mathrm{tr}(\dot{e}^{p3})}{[\mathrm{tr}(\dot{e}^{p2})]^{3/2}} \quad (4.5)$$

are the invariants of the plastic strain rate tensor $\dot{\boldsymbol{\epsilon}}^p$, $\dot{e}^p = \mathrm{dev}(\dot{\boldsymbol{\epsilon}}^p)$ is its deviatoric part, and θ_ϵ is the Lode angle of $\dot{\boldsymbol{\epsilon}}^p$

iii) the yield function (and the plastic potential, if any) depends on the stress tensor $\boldsymbol{\sigma}$ only through its invariants, i.e.:

$$f(\boldsymbol{\sigma}, \boldsymbol{\chi}; \boldsymbol{\zeta}) = \tilde{f}(p, q, z, \boldsymbol{\chi}; \boldsymbol{\zeta}) \qquad (4.6)$$

where

$$p = \frac{1}{3}\mathrm{tr}(\boldsymbol{\sigma}), \quad q = \left[\frac{3}{2}\mathrm{tr}(\boldsymbol{s}^2)\right]^{\frac{1}{2}}, \quad z = \sin(3\theta) = \sqrt{6}\frac{\mathrm{tr}(\boldsymbol{s}^3)}{[\mathrm{tr}(\boldsymbol{s}^2)]^{3/2}} \quad (4.7)$$

$\boldsymbol{s} = \mathrm{dev}(\boldsymbol{\sigma})$ is the stress deviator and θ is the Lode angle of the stress tensor $\boldsymbol{\sigma}$;

iv) the flow rules (2.13) and (3.3) imply the coaxiality between the stress and plastic strain rate tensors, see, e.g., [4].

v) due to (iv), the expression (2.8) for $\mathcal{D}$ can be written as

$$\mathcal{D} = p\dot{\epsilon}_v^p + q\dot{\epsilon}_s^p \cos\left(\theta - \theta_\epsilon\right) + \boldsymbol{\chi} \cdot \dot{\boldsymbol{\xi}} \qquad (4.8)$$

At yield, the stresses can be obtained from the dual flow rule (3.19), i.e., by differentiating the dissipation function. In the isotropic case, we obtain from (4.8)

$$p_y = \hat{p}_y(\dot{\epsilon}_v^p, \dot{\epsilon}_s^p, z_\epsilon) = \frac{1}{3}\mathrm{tr}\left(\frac{\partial\mathcal{D}}{\partial\dot{\boldsymbol{\epsilon}}^p}\right) = \frac{\partial\mathcal{D}}{\partial\dot{\epsilon}_v^p} \qquad (4.9)$$

$$q_y = \hat{q}_y(\dot{\epsilon}_v^p, \dot{\epsilon}_s^p, z_\epsilon) = \left[\frac{3}{2}\mathrm{tr}\left(\boldsymbol{s}_y^2\right)\right]^{1/2} \qquad (4.10)$$

$$z_y = \hat{z}_y(\dot{\epsilon}_v^p, \dot{\epsilon}_s^p, z_\epsilon) = \sqrt{6}\frac{\mathrm{tr}(\boldsymbol{s}_y^3)}{[\mathrm{tr}(\boldsymbol{s}_y^2)]^{3/2}} \qquad (4.11)$$

where

$$\boldsymbol{s}_y := \mathrm{dev}\left(\frac{\partial\mathcal{D}}{\partial\dot{\boldsymbol{\epsilon}}^p}\right).$$

13

4.2 Dependence on Lode angles

In order to develop a full three–invariant formulation, we will restrict attention to situations in which function $\hat{z}_y$ of (4.11) is of special form. We assume that z_y depends only on z_ϵ, i.e.:

$$z_y = \hat{z}(z_\epsilon) \tag{4.12}$$

and that $\hat{z}$ is invertible:

$$z_\epsilon = \hat{z}_\epsilon(z_y) \tag{4.13}$$

These assumptions turn out to be satisfied under relatively mild restrictions for the specific functional form (4.6) assumed for the yield surface, and are verified in a very large class of elasto–plastic models for soils. Essentially, the assumption is consistent with yield functions of the form (4.14), giving rise to a convex yield locus. This is detailed in the following two propositions.

Proposition 4.1. *An associative flow rule with a yield function of the form*

$$\tilde{f}(p, q, z, \chi; \zeta) = f\left(p, \frac{q}{M(z)}, \chi; \zeta\right), \tag{4.14}$$

where $M(z)$ is a scalar function of the third invariant of the stress tensor z, implies that the third invariant of the plastic strain rate tensor z_ϵ depends only on z.

Proof. The general definition of z_ϵ, eq. $(4.5)_3$, requires the evaluation of the scalar invariants $\mathrm{tr}(\dot{e}^{p2})$, $\mathrm{tr}(\dot{e}^{p3})$ of $\dot{e}^p$. In view of (4.14), and of the associative flow rule (3.3), we have

$$\dot{e}^p = \frac{\partial \tilde{f}}{\partial q}\frac{\partial q}{\partial \boldsymbol{\sigma}} + \frac{\partial \tilde{f}}{\partial z}\frac{\partial z}{\partial \boldsymbol{\sigma}} = \frac{\partial f}{\partial q^*}(\boldsymbol{B}_1 + \boldsymbol{B}_2) \tag{4.15}$$

where $q^* := q/M(z)$ and

$$\boldsymbol{B}_1 := \frac{\partial q^*}{\partial q}\frac{\partial q}{\partial \boldsymbol{\sigma}} \qquad\qquad \boldsymbol{B}_2 := \frac{\partial q^*}{\partial z}\frac{\partial z}{\partial \boldsymbol{\sigma}} \tag{4.16}$$

are two symmetric second order tensors, both coaxial with $\boldsymbol{\sigma}$, which are homogeneous functions of degree zero in $\boldsymbol{\sigma}$ and independent of the specific choice for the yield function f. It follows that

$$\mathrm{tr}(\dot{e}^{p2}) = \left(\frac{\partial f}{\partial q^*}\right)^2 b_1 \tag{4.17}$$

$$\mathrm{tr}(\dot{e}^{p3}) = \left(\frac{\partial f}{\partial q^*}\right)^3 b_2 \tag{4.18}$$

where, since $\boldsymbol{B}_1$ and $\boldsymbol{B}_2$ commute, the scalar functions b_1 and b_2 are given by

$$b_1 = \mathrm{tr}\left(\boldsymbol{B}_1^2 + \boldsymbol{B}_2^2 + 2\boldsymbol{B}_1\boldsymbol{B}_2\right) \tag{4.19}$$

$$b_2 = \mathrm{tr}\left(\boldsymbol{B}_1^3 + 3\boldsymbol{B}_1^2\boldsymbol{B}_2 + 3\boldsymbol{B}_1\boldsymbol{B}_2^2 + \boldsymbol{B}_2^3\right) \tag{4.20}$$

In principle, b_1 and b_2 could depend on the stress tensor through both second and third invariant. However, since $\boldsymbol{B}_1$ and $\boldsymbol{B}_2$ are homogeneous of degree zero

in $\boldsymbol{\sigma}$, so have to be both b_1 and b_2. Thus, dependence on q is ruled out. In fact, a lengthy but otherwise straightforward calculation shows that, for every possible choice of the yield function f,

$$b_1 = \frac{1}{M^2} \left\{ \frac{3}{2} + \frac{2}{27}(1-z^2) \left(\frac{M'}{M} \right)^2 \right\} \tag{4.21}$$

$$b_2 = \frac{3}{4M^3} \left\{ z - 9(1-z^2)\frac{M'}{M} - 27z(1-z^2) \left(\frac{M'}{M} \right)^2 + 27(1-z^2)^2 \left(\frac{M'}{M} \right)^3 \right\} \tag{4.22}$$

Thus, plugging (4.17) and (4.18) into eq. $(4.5)_3$, we obtain

$$z_\epsilon = \hat{z}_\epsilon(z) = \sqrt{6}\frac{b_2(z)}{[b_1(z)]^{3/2}} \tag{4.23}$$

as claimed. $\qquad\square$

Remark 4.1. Proposition 4.1 can be extended to the case of a non–associative flow rule (2.13), provided that the plastic potential g has the same dependence on q and z as the one assumed for the yield function f, see eq. (4.14).

Invertibility of the function $\hat{z}_\epsilon$ is guaranteed if the trace of the yield locus on the deviatoric plane is a convex curve, as proved below.

Proposition 4.2. *Assume that the yield locus $\{f = 0\}$ is convex, so that each deviatoric section is convex and, in particular, the curve defined by the following parametric representation*

$$z \mapsto \{R(z)\cos\Theta(z), R(z)\sin\Theta(z)\} \qquad z \in [-1,1] \tag{4.24}$$

where

$$R(z) := \sqrt{\frac{2}{3}}q(z) \qquad\qquad \Theta(z) := \frac{1}{3}\left[\pi + \sin^{-1}(z)\right]$$

and $q(z)$ is defined implicitly by the equation

$$f(p_0, \frac{q}{M(z)}, \boldsymbol{\chi}_0; \boldsymbol{\zeta}_0) = 0 \qquad\qquad (\text{for } p_0, \boldsymbol{\chi}_0, \boldsymbol{\zeta}_0 \text{ given})$$

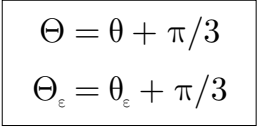*is convex. Then the function $\hat{z}_\epsilon$ is invertible.*

Proof. Equation (4.24) gives the representation of the deviatoric section $\mathcal{C}$ of the yield locus at $p = p_0$ in polar coordinates (note that $\Theta = \pi/3 + \theta$). The unit vector normal to the curve (which has the direction of the deviatoric part of the plastic strain increment) is given by

$$\boldsymbol{N}_p = (\cos\Theta_\epsilon, \sin\Theta_\epsilon) , \quad \Theta_\epsilon := \frac{\pi}{3} + \theta_\epsilon . \tag{4.25}$$

Denoting arc-length by s, one has that the curvature κ of $\mathcal{C}$ is given by

$$\kappa(s) = \frac{d}{ds}\Theta_\epsilon(s) = \frac{d}{ds}\theta_\epsilon(s) , \tag{4.26}$$

see [20]. For the convex curve $\mathcal{C}$, $\kappa(s)$ has a fixed sign (say, strictly positive), hence $\Theta_\epsilon(s)$ is invertible. This shows that $\mathcal{C}$ admits a paremetrization in terms of the normal angle $\Theta_\epsilon = [\pi + \sin^{-1}(z_\epsilon)]/3$. This establishes a one-to-one correspondence between the parameter z in (4.24) and z_ϵ, as claimed. $\qquad\square$

15

Figure 4: Deviatoric section of the yield surface at $p = p_0$. In view of symmetry, only the sector with Lode angle $\theta \in (-\pi/6, \pi/6)$, i.e., $\Theta \in (\pi/6, \pi/2)$ is shown.

The link between the Lode angles of stress and plastic strain rate introduced by eqs. (4.12) and (4.13) allows us to construct the yield locus section–wise. First, sections at $z = $ const., can be obtained by setting $z_\epsilon = $ const. in the appropriate derivatives of the dissipation function, see eqs. (4.9) and (4.10); second, the shape of the yield locus on the deviatoric plane can be defined by prescribing function $\hat{z}$ or its inverse $\hat{z}_\epsilon$ in eqs. (4.12) and (4.13).

The homogeneity properties of $\mathcal{D}$ force p_y and q_y to be homogenous functions of degree zero in $\dot{\epsilon}^p$. Hence the functions $\hat{p}_y$ and $\hat{q}_y$ in eqs. (4.9) and (4.10) are homogeneous functions of degree zero in the invariants $\dot{\epsilon}_v^p$ and $\dot{\epsilon}_s^p$. In particular, we assume

$$p_y = p_{y,\epsilon}(\delta) = \tilde{p}_y(\delta, z_\epsilon) \tag{4.27}$$

$$q_y = q_{y,\epsilon}(\delta) = \tilde{q}_y(\delta, z_\epsilon) \tag{4.28}$$

in which the function δ, defined as:

$$\delta := \frac{1}{\cos(\theta - \theta_\epsilon)} \frac{\dot{\epsilon}_v^p}{\dot{\epsilon}_s^p} \tag{4.29}$$

is a generalization of the classical definition of the dilatancy

$$d := \frac{\dot{\epsilon}_v^p}{\dot{\epsilon}_s^p} \tag{4.30}$$

employed in axisymmetric stress and deformation states (for which $\theta = \theta_\epsilon$).

Eqs. (4.27) and (4.28) mean that the meridian sections of the yield locus (i.e., sections at $z = $ const.) can be parametrized by the dilatancy δ. This is always the case for a convex yield locus, as shown in the following proposition.
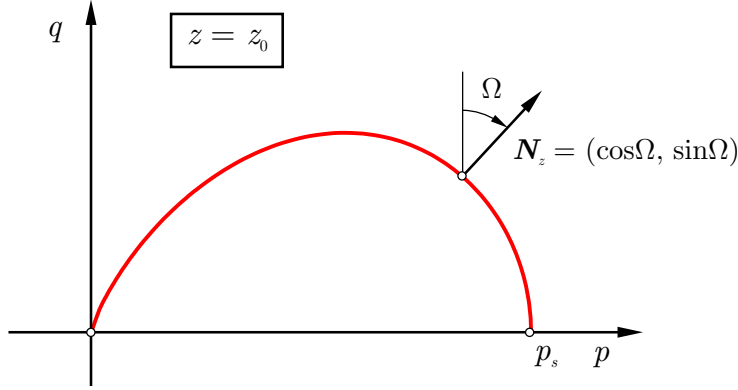
16

Figure 5: Meridian section of the yield surface in $q : p$ plane, for $z = z_0$. The angle Ω is defined by $\Omega := \tan^{-1} \delta$, where δ is the dilatancy.

Proposition 4.3. *Assume that the yield locus $\{f = 0\}$ is convex, so that each meridian section is convex and, in particular, the one at $z = z_0$ defined by the following parametric representation*

$$p \mapsto q(p) \qquad\qquad p \in [0, p_{\max}] \qquad\qquad (4.31)$$

where $q(p)$ is defined implicitly by the equation

$$f\left(p, \frac{q}{M(z_0)}, \chi_0; \zeta_0\right) = 0 \qquad\qquad \text{for } z_0, \, \chi_0, \, \zeta_0 \text{ given}$$

is a convex curve. Then each meridian section admits a parametrization in terms of the dilatancy δ.

Proof. The proof follows from the same argument used in proposition 4.2, i.e., that a convex curve can be parametrized in terms of the normal angle. The unit normal vector $\boldsymbol{N}_z$ to the meridian section at $z = z_0$ is proportional to $(\dot{\epsilon}_v^p, \Gamma_0 \dot{\epsilon}_s^p)$, where $\Gamma_0 = \cos[\theta(z_0) - \theta_\epsilon(z_0)]$, hence

$$\boldsymbol{N}_z = (\sin\Omega, \cos\Omega), \quad \Omega := \tan^{-1}\delta. \qquad\qquad (4.32)$$

Thus, a parametrization in terms of the normal angle $\pi/2 - \Omega$ induces a parametrization in terms of the dilatancy δ. $\qquad\qquad\square$

4.3 Construction of yield locus from stress–dilatancy and dual flow rule

For each fixed z_ϵ, equations (4.27) and (4.28) define parametrically a $\theta = $ constant section of the yield locus

$$\delta \mapsto \{p_{y,\epsilon}(\delta), q_{y,\epsilon}(\delta)\}. \qquad\qquad (4.33)$$

We want to eliminate parameter δ from the previous expression, to obtain a representation of the yield locus in the form

$$(p_y, z) \mapsto q_y = \bar{q}(p_y, z). \qquad\qquad (4.34)$$

17

In order to proceed, let us first notice that equations (4.27) and (4.28) imply the existence of a stress–dilatancy relation of the form

$$\eta := \frac{q_y}{p_y} = \Phi(\delta, z_\epsilon) =: \Phi_\epsilon(\delta) \,, \tag{4.35}$$

where η is the stress ratio q_y/p_y at yield and the third identity simply defines a shorthand notation for function $\Phi(\delta, z_\epsilon)$. With (4.35), the dissipation function (4.8) can be rewritten as:

$$\mathcal{D} = \mathcal{D}_p + \boldsymbol{\chi} \cdot \dot{\boldsymbol{\xi}} = \Sigma_\epsilon(\delta)\Gamma(z_\epsilon)\dot{\epsilon}_s^p + \boldsymbol{\chi} \cdot \dot{\boldsymbol{\xi}} \tag{4.36}$$

where

$$\mathcal{D}_p := \boldsymbol{\sigma} \cdot \dot{\boldsymbol{\epsilon}}^p = \Sigma_\epsilon(\delta)\Gamma(z_\epsilon)\dot{\epsilon}_s^p \tag{4.37}$$

is the plastic power density and

$$\Sigma_\epsilon(\delta) = \Sigma(\delta, z_\epsilon) := p_{y,\epsilon}(\delta)\left[\delta + \Phi_\epsilon(\delta)\right] \tag{4.38}$$
$$\Gamma(z_\epsilon) := \cos(\theta - \theta_\epsilon) \,. \tag{4.39}$$

Expressions similar to eq. (4.36) above are discussed in [21].

From (4.9) and (4.37), we have

$$p_y = \frac{\partial \mathcal{D}}{\partial \dot{\epsilon}_v^p} = \frac{\partial \mathcal{D}_p}{\partial \delta}\frac{\partial \delta}{\partial \dot{\epsilon}_v^p} = \Sigma_\epsilon'(\delta) \tag{4.40}$$

having used the fact that

$$\frac{\partial \delta}{\partial \dot{\epsilon}_v^p} = \frac{1}{\Gamma \dot{\epsilon}_s^p} \,. \tag{4.41}$$

More explicitly, differentiating (4.38) with respect to δ

$$\Sigma_\epsilon'(\delta) = \left[\delta + \Phi_\epsilon(\delta)\right] p_{y,\epsilon}'(\delta) + \left[1 + \Phi_\epsilon'(\delta)\right] p_{y,\epsilon}(\delta) \,, \tag{4.42}$$

we obtain from (4.40)

$$(\delta + \Phi_\epsilon)\, p_{y,\epsilon}' + \Phi_\epsilon' p_{y,\epsilon} = 0 \,, \tag{4.43}$$

an ordinary differential equation (ODE) in the unknown function

$$\delta \mapsto p_{y,\epsilon}(\delta) \tag{4.44}$$

For each fixed z_ϵ, (4.43) may be solved and function (4.44) may be inverted to give

$$\delta = \delta_\epsilon(p_y) = \delta(p_y, z_\epsilon) \,. \tag{4.45}$$

Plugging this into (4.35), and assigning the function $z_\epsilon = z_\epsilon(z)$, we obtain

$$q_y = p_y \Phi\left(\delta(p_y, z_\epsilon(z)), z_\epsilon(z)\right) = \bar{q}(p_y, z) \,, \tag{4.46}$$

as desired. The procedure is summarized in Box 3.

In practice, since an experimental identification of the function $z_\epsilon = z_\epsilon(z)$ is far from trivial, we determine (4.46) for $z_\epsilon = z = \pm\pi/6$ (uniaxial compression and extension, the two cases accessible with the use of a standard triaxial apparatus), and then assign the dependence on z by prescribing the function $z \mapsto M(z)$ in (4.14) consistently with the requirement that the yield locus should be convex, e.g., à la van Eekelen [55].

18

Box 3. Yield locus from stress-dilatancy relation (two-invariant theory, $\theta_\epsilon \equiv \theta$, is recovered with $\Gamma := \cos(\theta - \theta_\epsilon) \equiv 1$ and dropping subscript ϵ).

$$\delta = \frac{\dot{\epsilon}_v^p}{\Gamma \dot{\epsilon}_s^p} \qquad\qquad\qquad \text{dilatancy}$$

$$\frac{q_y}{p_y} = \Phi_\epsilon(\delta) \qquad\qquad\qquad \text{stress–dilatancy}$$

$$p_y = p_{y,\epsilon}(\delta)\,, \quad q_y = q_{y,\epsilon}(\delta) \qquad\qquad \text{convexity of yield locus}$$

$$\mathcal{D}_p = \boldsymbol{\sigma} \cdot \dot{\boldsymbol{\epsilon}}^p = \Sigma_\epsilon(\delta)\Gamma\dot{\epsilon}_s^p \qquad\qquad \text{plastic power using stress–dilatancy}$$

$$p_y = \frac{\partial \mathcal{D}_p}{\partial \delta}\frac{\partial \delta}{\partial \dot{\epsilon}_v^p} = \Sigma_\epsilon'(\delta) \qquad\qquad \text{dual flow rule, eq. (4.40)}$$

$$\Sigma_\epsilon' = [\delta + \Phi_\epsilon]\,p_{y,\epsilon}' + [1 + \Phi_\epsilon']\,p_{y,\epsilon} \qquad \text{eq. (4.42), from } \Sigma_\epsilon := [\delta + \Phi_\epsilon]\,p_{y,\epsilon}$$

$$[\delta + \Phi_\epsilon]\,p_{y,\epsilon}' + \Phi_\epsilon' p_{y,\epsilon} = 0 \qquad\qquad \text{ODE in } \delta \mapsto p_{y,\epsilon}, \text{ from } (4.40),(4.42)$$

$$\delta_\epsilon(p_y) \qquad\qquad\qquad \text{inverse of } \delta \mapsto p_{y,\epsilon}$$

$$q_y = p_y \Phi_\epsilon(\delta_\epsilon(p_y)) \qquad\qquad\qquad \text{yield locus}$$

Remark 4.2. The explicit expression of the plastic dissipation in terms of plastic strain rates can be obtained by plugging the solution $\delta \mapsto p_{y,\epsilon}(\delta)$ into the expression (4.37) for $\mathcal{D}_p$. This becomes a function of the plastic strain rates through δ, $\dot{\epsilon}_s^p$, and z_ϵ

$$\mathcal{D}_p = p_y(\delta, z_\epsilon)\,[\delta + \Phi(\delta, z_\epsilon)]\,\Gamma(z_\epsilon)\dot{\epsilon}_s^p \tag{4.47}$$

which can, in principle, be used to derive z_y by differentiation with the use of the dual flow rule (4.11).

4.4   Examples

As an example, consider the linear stress–dilatancy relation

$$\eta = M - \frac{1}{m}\delta \qquad\qquad \delta = m(M - \eta)\,, \tag{4.48}$$

i.e., a relation of the form (4.35), in which function Φ_ϵ is given by

$$\Phi_\epsilon(\delta) = \Phi(\delta, z_\epsilon) = M(z_\epsilon) - \frac{1}{m}\delta\,. \tag{4.49}$$

Here m and M are material parameters representing, respectively, the slope of the stress–dilatancy line in the $\delta : \eta$ plane and its intercept on the η axis. Substituting into the ODE (4.43), we obtain

$$\left[M - \frac{1}{m}\delta + \delta\right]p_{y,\epsilon}' - \frac{1}{m}\,p_{y,\epsilon} = 0\,, \tag{4.50}$$

19

i.e.,
$$[mM + (m-1)\delta]\, p'_{y,\epsilon} - p_{y,\epsilon} = 0\,. \tag{4.51}$$
This is easily integrated to give
$$p_y(\delta, z_\epsilon) = p_s \left[\frac{m-1}{m}\frac{1}{mM}\,\delta + \frac{1}{m}\right]^{\frac{1}{m-1}}\,, \quad m \neq 1\,, \tag{4.52}$$
where p_s is the value of p_y corresponding to the maximal dilatancy $\delta = mM$ compatible with (4.48) and positivity of q. Note that p_s gives the intercept of the yield locus with the axis of isotropic compression, and the yield locus must be a closed surface. Therefore the integration constant p_s, which in principle should depend on z_ϵ, must in fact be independent of the Lode angle.

Inverting expression (4.52) giving p_y as a function of δ we obtain
$$\delta(p_y, z_\epsilon) = \left[\left(\frac{p_y}{p_s}\right)^{m-1} - \frac{1}{m}\right]\frac{m^2 M}{m-1}\,, \quad m \neq 1\,, \tag{4.53}$$
and hence, substituting into (4.48),
$$q_y = M(z_\epsilon) p_y \frac{m}{m-1}\left[1 - \left(\frac{p_y}{p_s}\right)^{m-1}\right]\,, \quad m \neq 1\,. \tag{4.54}$$

Remark 4.3. Define p_0 as the value of p_y corresponding to null dilatancy:
$$p_0 = p_y(\delta, z_\epsilon)|_{\delta=0} \tag{4.55}$$
Then the ratio between p_0 and p_s
$$\frac{p_0}{p_s} = \left(\frac{1}{m}\right)^{\frac{1}{m-1}} \tag{4.56}$$
is independent of the Lode angle, provided that m is independent of z_ϵ.

Remark 4.4. Assuming M independent of z_ϵ, and taking $m = 1$ in (4.48) gives the stress–dilatancy relation
$$\frac{q_y}{p_y} = M - \delta \tag{4.57}$$
of the original Cam Clay model. The relation between p_y and δ is, in this case,
$$p_y(\delta) = p_s \exp\left(\frac{\delta}{M} - 1\right) \tag{4.58}$$
and the corresponding yield locus is obtained by taking the limit $m \to 1$ in (4.54) leading to
$$q_y = M p_y \ln\left(\frac{p_y}{p_s}\right)\,. \tag{4.59}$$

The explicit expression (4.47) of the dissipation $\mathcal{D}_p$ as a function of the plastic strain and strain rates has been obtained in [37] and is given by
$$\mathcal{D}_p = p_y(\delta) M \dot{\epsilon}_s^p = p_s \exp\left(\frac{\delta}{M} - 1\right) M \dot{\epsilon}_s^p\,. \tag{4.60}$$

Typically, it is assumed that $p_s = p_s(\epsilon_v^p) = \bar{p}_s \exp\left(\rho_s(\epsilon_v^p - \bar{\epsilon}_v^p)\right)$ consistently with the classical (non-associative) volumetric hardening law $\dot{p}_s = \rho_s p_s \dot{\epsilon}_v^p$.

As a second example, we consider the model proposed in [32] starting from the stress-dilatancy relation

$$\delta = m \, (M - \eta) \left(1 + a \frac{M}{\eta} \right) , \qquad (4.61)$$

where a is a dimensionless (regularization) parameter, typically much smaller than one. The corresponding yield function is

$$f = A^{K_1/C} B^{-K_2/C} p - p_s , \qquad (4.62)$$

where

$$A(p, q, \theta) := 1 + \frac{1}{K_1 M(\theta)} \frac{q}{p} \qquad (4.63)$$

$$B(p, q, \theta) := 1 + \frac{1}{K_2 M(\theta)} \frac{q}{p} \qquad (4.64)$$

$$C := (1 - m)(K_1 - K_2) \qquad (4.65)$$

$$K_1 := \frac{m(1 - a)}{2(1 - m)} \left\{ 1 + \sqrt{1 - \frac{4a(1 - m)}{m(1 - a)^2}} \right\} \qquad (4.66)$$

$$K_2 := \frac{m(1 - a)}{2(1 - m)} \left\{ 1 - \sqrt{1 - \frac{4a(1 - m)}{m(1 - a)^2}} \right\} \qquad (4.67)$$

$$M(\theta) := c_1 [1 + c_2 \sin(3\theta)]^n \, M_c \qquad (4.68)$$

and c_1, c_2 and n are material constants. The quantities c_1 and c_2 can be expressed as functions of the ratio $c_M := M_e / M_c$ between the values taken by the function $M(\theta)$ in axisymmetric extension ($\theta = -\pi/6$) and axisymmetric compression ($\theta = \pi/6$):

$$c_1 := \frac{1}{2^n} [1 + (c_M)^{1/n}]^n \qquad\qquad c_2 := \frac{1 - (c_M)^{1/n}}{1 + (c_M)^{1/n}} . \qquad (4.69)$$

Equation (4.69) defines the dependence of the stress ratio at critical state on the Lode angle. It has been proposed by van Eekelen in [55], where the conditions ensuring the convexity of the deviatoric section of the resulting yield locus are also discussed.

4.5 Remarks on stress–dilatancy relations

We have made systematic use of stress–dilatancy relations, i.e., of relations of the form

$$\eta = \frac{q_y}{p_y} = \Phi(\delta) \qquad (4.70)$$

or of the form

$$\delta = \frac{\dot{\epsilon}_v^p}{\dot{\epsilon}_s^p} = \Delta(\eta) . \qquad (4.71)$$

Here, and throughout this subsection, we restrict our discussion to the axisymmetric case [i.e., $\Gamma \equiv 1$ in (4.39)] for the sake of simplicity. The relevance of

relations of this kind in describing the observed stress–strain behavior of geo-materials goes back a long way, see e.g. [48], [49], [51], [52]. Stress–dilatancy relations have been measured experimentally for a wide range of both natural and artificial granular materials, and they have been extensively used in the development of constitutive models, see Box 4.

Relation (4.71) expresses the dependence of plastic strain rates from the current stress. Thus, it is conceptually a flow rule. In fact, referring to the non-associative expression (2.13) for greater generality, it is a relation of the form

$$\frac{\dot{\epsilon}_v^p}{\dot{\epsilon}_s^p} = \left.\frac{\partial g/\partial p}{\partial g/\partial q}\right|_{g=0} = \Delta\left(\frac{q}{p}\right). \tag{4.72}$$

Assuming that the set $\{g = 0\}$ in the $q : p$ plane can be described as the graph of a function $p \mapsto \bar{q}(p)$, i.e.,

$$\{(p, q) : g(p, q) = 0\} = \{(p, q) : q = \bar{q}(p)\} \tag{4.73}$$

we can rewrite (4.72) in the form

$$\bar{q}'(p) = \Delta\left(\frac{\bar{q}(p)}{p}\right). \tag{4.74}$$

Integrating this ODE one can determine $\bar{q}$ and hence the zero level set $\{g = 0\}$ of the plastic potential. In the associative case $f = g$, and the same procedure leads to the determination of the yield locus $\{f = 0\}$. This is the approach most commonly used in CSSM.

Relation (4.70) expresses the dependence of yield stresses on the corresponding plastic strain rates. Thus, it is conceptually a dual flow rule. More precisely, it is (4.10) which, in the axisymmetric case, reads as

$$q_y = p_y \Phi(\delta) = \frac{\partial \mathcal{D}_p}{\partial \dot{\epsilon}_s^p}. \tag{4.75}$$

Indeed, we have from (4.37) that $\mathcal{D}_p = \Sigma(\delta)\dot{\epsilon}_s^p$, where $\Sigma = [\delta + \Phi]\, p_y$, and hence

$$\frac{\partial \mathcal{D}_p}{\partial \dot{\epsilon}_s^p} = \frac{\partial}{\partial \dot{\epsilon}_s^p}\left(\Sigma(\delta)\dot{\epsilon}_s^p\right) = \Sigma(\delta) - \Sigma'(\delta)\delta, \tag{4.76}$$

having used the fact that

$$\frac{\partial \delta}{\partial \dot{\epsilon}_s^p} = -\frac{1}{\dot{\epsilon}_s^p}\delta. \tag{4.77}$$

The right hand side of (4.76) is in turn

$$[\delta + \Phi]\, p_y - p_y\delta - \left\{[\delta + \Phi]p_y' + \Phi'p_y\right\}\delta = p_y\Phi, \tag{4.78}$$

because p_y solves the ODE (4.43), hence proving the claim.

Solution of the ODE (4.43) is anyway necessary to obtain δ as a function of p_y and to arrive, by substitution into (4.75), at the explicit expression of the yield locus as the graph of a function $p_y \mapsto \bar{q}_y(p)$ in the $q : p$ plane.

Box 4. Yield functions and corresponding stress-dilatancy relations
(CC = original Cam–clay; MCC = modified Cam–clay).

model	yield function f	$\eta = \Phi(\delta)$ Φ	$\delta = \Delta(\eta)$ Δ
Ref. [53] (CC)	$\dfrac{q}{M} - p\ln\left(\dfrac{p}{p_s}\right)$	$M - \delta$	$M - \eta$
Ref. [44]	$\dfrac{q}{M} - \dfrac{mp}{1-m}\left[1 - \left(\dfrac{p}{p_s}\right)^{m-1}\right]$	$M - \dfrac{1}{m}\delta$	$m(M - \eta)$
Ref. [32]	$A^{K_1/C}B^{-K_2/C}p - p_s$ where $A = A\left(\dfrac{q}{M}\right),\, B = B\left(\dfrac{q}{M}\right)$	$\dfrac{1}{2}\left\{\left[P_\epsilon^2(\delta) + 4aM^2\right]^{\frac{1}{2}} + P_\epsilon(\delta)\right\},$ where $P_\epsilon(\delta) := (1-a)M - \dfrac{1}{m}\delta$	$m(M - \eta)\left(1 + \dfrac{aM}{\eta}\right)$
Ref. [47] (MCC)	$\left(\dfrac{q}{M}\right)^2 - p(p_s - p)$	$\left[\delta^2 + M^2\right]^{\frac{1}{2}} + \delta$	$\dfrac{1}{2}(M - \eta)\left(1 + \dfrac{M}{\eta}\right)$

5 The case of soils with crushable grains

The general approach outlined above can be applied in a straightforward manner to the development of associative plasticity models for granular materials

undergoing grain crushing, provided that the effects of grain crushing are accounted for by introducing a set of suitable (scalar) internal variables as, for example, in [8]. In fact, in the derivation of the yield function from a given dilatancy rule, the internal variables play the role of constants. Therefore, the procedure discussed in the previous sections can still be used to associate a family of yield loci to the assigned family of stress–dilatancy curves, parametrized by such internal variables.

The starting point of the phenomenological plasticity model presented in [8] is the stress–dilatancy relation (4.61), which, in the associative case corresponds to the yield function (4.62). Available experimental evidence suggests that the ultimate value of the friction angle at constant volume is an increasing function of the mean grain diameter (see, e.g., [25, 36]), and that the position of the virgin compression line (VCL), in the $\epsilon_v : \ln(p)$ plane, may also depend on the mean grain diameter [14]. These effects have been taken into account by Cecconi et al. by including the parameters M and m of eqs. (4.66)–(4.68) in the set of internal variables, and replacing the isotropic yield stress in compression, p_s, with $p_c = bp_s$, where $b \geq 1$ is an additional internal variable which allows to describe a downward translation of the isotropic virgin compression line as the material degrades. The evolution laws adopted for M, m and b are such that these quantities vary monotonically with increasing plastic strain magnitude, from their initial value to a final, ultimate value at a stable (asymptotic) state in which all grain–crushing phenomena are ceased. In the following, the same concepts are used to develop a thermodynamically consistent version of the same model.

5.1 Yield function and hardening laws

Following [8], we adopt as yield function a slight modification of (4.62), namely,

$$f(\boldsymbol{\sigma}, \chi_b, \chi_M; p_s) = \tilde{A}^{K_1/C} \tilde{B}^{-K_2/C} p \chi_b - p_s \tag{5.1}$$

where p_s, χ_b and χ_M represent the internal state variables,

$$\tilde{A} = 1 + \frac{1}{K_1} \frac{\chi_M q}{p} \tag{5.2}$$

$$\tilde{B} = 1 + \frac{1}{K_2} \frac{\chi_M q}{p} \tag{5.3}$$

and K_1, K_2, and $C = (1 - m)(K_1 - K_2)$ are defined in terms of the material constants m and a entering the stress–dilatancy equation (4.61) by eqs. (4.66) and (4.67)

By comparing eq. (4.62) (with p_s replaced by $p_c = bp_s$) with eq. (5.1) and eqs. (4.63)–(4.64) with eqs. (5.2)–(5.3) it is immediately apparent that the two quantities χ_b and χ_M can be interpreted as the inverse of the internal variables b and M of the Cecconi et al. [8] model:

$$\chi_b = \frac{1}{b} \qquad\qquad \chi_M = \frac{1}{M} \tag{5.4}$$

i.e., χ_b represents the ratio p_s/p_c between the yield stress in isotropic compression at the stable state, p_s, and the *current* yield stress in isotropic compression,

p_c, while χ_M is the inverse of the stress ratio at the critical state in axisymmetric compression ($\theta = \pi/6$).

The evolution equations for the plastic strain rate are provided by the associative flow rule (3.3). The model is completed by specifying hardening laws for parameters χ_M, χ_b, and p_s.

To endow the model with a thermodynamic structure, we consider the free energy function

$$\psi = \psi_e(\boldsymbol{\epsilon}^e) + \psi_M(\xi_M) + \psi_b(\xi_b) \tag{5.5}$$

where

$$\psi_e(\boldsymbol{\epsilon}^e) = \psi(\epsilon_v^e, \epsilon_s^e) = \tilde{\psi}(\epsilon_v^e) + \frac{3}{2}G_0(\epsilon_s^e)^2 \tag{5.6}$$

$$\psi_M(\xi_M) = -\chi_{M,\infty}\xi_M + \frac{\chi_{M,\infty} - \chi_{M,0}}{\rho_M}\left\{1 - \exp(-\rho_M\xi_M)\right\} \tag{5.7}$$

$$\psi_b(\xi_b) = -\xi_b + \frac{1 - \chi_{b,0}}{\rho_b}\left\{1 - \exp(-\rho_b\,\xi_b)\right\} \tag{5.8}$$

and function $\tilde{\psi}(\epsilon_v^e)$ is given by

$$\tilde{\psi}(\epsilon_v^e) := \begin{cases} \hat{\kappa}p_r\exp\left(\epsilon_v^e/\hat{\kappa} - 1\right) & (\epsilon_v^e \geq \hat{\kappa}) \\ p_r\epsilon_v^e + p_r\left(\epsilon_v^e - \hat{\kappa}\right)^2/(2\hat{\kappa}) & (\epsilon_v^e < \hat{\kappa}) \end{cases} \tag{5.9}$$

In eqs. (5.6)–(5.9), p_r, $\hat{\kappa}$, G_0, ρ_M, $\chi_{M,0}$, $\chi_{M,\infty}$, ρ_b and $\chi_{b,0}$ are material constants[3].

The yield locus described by function (5.1) follows from a dissipation function of the form

$$\mathcal{D} = \mathcal{D}_p + \boldsymbol{\chi} \cdot \dot{\boldsymbol{\xi}} = \Sigma_\epsilon(\delta)\Gamma(z_\epsilon)\dot{\epsilon}_s^p + \chi_M\dot{\xi}_M + \chi_b\dot{\xi}_b \,. \tag{5.10}$$

Here $\Sigma_\epsilon = [\delta + \Phi_\epsilon]\,p_{y,\epsilon}$ where Φ_ϵ, obtained from the stress–dilatancy relation (4.61), is given by

$$\Phi_\epsilon = \frac{1}{2}\left\{\left[P_\epsilon^2(\delta) + 4aM^2\right]^{\frac{1}{2}} + P_\epsilon(\delta)\right\} \tag{5.11}$$

$$P_\epsilon(\delta) := (1-a)M - \frac{1}{m}\delta \,. \tag{5.12}$$

while χ_M and χ_b are given by

$$\chi_M = -\psi_M'(\xi_M) = \chi_{M,\infty} - (\chi_{M,\infty} - \chi_{M,0})\exp(-\rho_M\xi_M) \tag{5.13}$$

$$\chi_b = -\psi_b'(\xi_b) = 1 - (1 - \chi_{b,0})\exp(-\rho_b\xi_b) \,. \tag{5.14}$$

Clearly,

$$\chi_{M,\infty} \geq \chi_{M,0} > 0 \quad , \quad 1 = \chi_{b,\infty} \geq \chi_{b,0} > 0 \,. \tag{5.15}$$

---

[3]According to eq. (5.9), for $\epsilon_v^e \geq \hat{\kappa}$ the free energy function (5.6) describes a pressure–dependent, hyperelastic behaviour, with a constant shear modulus G_0 and a bulk modulus $K = p/\hat{\kappa}$. For $\epsilon_v^e < \hat{\kappa}$, the stored energy function reduces to the classical quadratic expression of linear elasticity. Eq. (5.6) is a simplified version of the stored energy function proposed by Houlsby, see e.g., [27]. The minor modification introduced with the switch condition (5.9) allows to extend the validity of the original model to the tensile stress range.

In view of (3.6), we get from eqs. (5.11) and (5.12) the associative hardening laws

$$\dot\chi_M = \dot\gamma\,\rho_M\,(\chi_{M,\infty} - \chi_M)\,\frac{\partial f}{\partial\chi_M} \tag{5.16}$$

$$\dot\chi_b = \dot\gamma\,\rho_b\,(1 - \chi_b)\,\frac{\partial f}{\partial\chi_b}\,. \tag{5.17}$$

Remark 5.1. In view of the additive structure of ψ^p in (5.5), which uncouples the two hardening mechanisms, tensor $\mathbb{D}_\xi(\boldsymbol\xi) = \partial^2\psi^p/(\partial\boldsymbol\xi\otimes\partial\boldsymbol\xi)$ is diagonal. Notice also that, since

$$\frac{\partial f}{\partial q} = \frac{\chi_b\chi_M}{C}\,A^{K_1/C}\,B^{-K_2/C}(A^{-1} - B^{-1}) \tag{5.18}$$

and

$$\frac{\partial f}{\partial\chi_M} = \frac{\chi_b q}{C}\,A^{K_1/C}\,B^{-K_2/C}(A^{-1} - B^{-1}) = \frac{q}{\chi_M}\,\frac{\partial f}{\partial q} \tag{5.19}$$

we have

$$\dot\chi_M = \rho_M\frac{\chi_{M,\infty} - \chi_M}{\chi_M}\,q\,\dot\epsilon_s^p. \tag{5.20}$$

This is a purely deviatoric hardening law showing that, within our associative model, the rate of change of χ_M is proportional to the distortional plastic power. On the other hand, from

$$\frac{\partial f}{\partial p} = \chi_b\,A^{K_1/C}B^{-K_2/C}\left\{1 - \frac{\chi_M q}{p\,C}[A^{-1} - B^{-1}]\right\} \tag{5.21}$$

$$\frac{\partial f}{\partial\chi_b} = A^{K_1/C}B^{-K_2/C}p \geqslant 0 \tag{5.22}$$

we get

$$\frac{\partial f}{\partial\chi_b} = \frac{p}{\chi_b}\,\frac{\partial f}{\partial p} + \frac{q}{\chi_b}\,\frac{\partial f}{\partial q} \tag{5.23}$$

and, in turn,

$$\dot\chi_b = \rho_b\,\frac{1 - \chi_b}{\chi_b}\,\{p\dot\epsilon_v^p + q\dot\epsilon_s^p\} \tag{5.24}$$

Thus, in the associative case, the rate of change of χ_b depends on both the volumetric and the deviatoric components of the plastic power. In particular, in axisymmetric conditions ($\Gamma = 1$), the rate at which $\frac{1}{b}$ evolves is proportional to the plastic power. A consequence of the associativity of the proposed hardening laws is that, in an isotropic compression experiment ($q = 0$), $\dot\chi_M$ vanishes because $\dot\epsilon_s^p = 0$.

Remark 5.2. The evolution laws (5.16) and (5.17) are consistent with the phenomenological hardening laws employed in [8] for M and b. They describe a monotonic decay of parameters M and b from the initial values $M_0 = (\chi_{M,0})^{-1}$ and $b_0 = (\chi_{b,0})^{-1}$ to the final asymptotic values $M_\infty = (\chi_{M,\infty})^{-1}$ and $b_\infty =$

Table 1: Material parameters for the Pozzolana Nera.

$\hat{\kappa}$	0.002	a	0.001
G_0 (kPa)	$2.5 \cdot 10^5$	m	2.0
p_r (kPa)	400.0	ρ_s	14.0
$\chi_{M,\infty}$	0.625	ρ_M	$1.0 \cdot 10^{-3}$
c_M	0.652	ρ_b	$2.0 \cdot 10^{-5}$

$(\chi_{b,\infty})^{-1} = 1$ *as grain crushing proceeds. Notice, however, that while in our approach the quantity m is a material constant, in [8] m evolves together with M so that*

$$mM = \text{const.} \tag{5.25}$$

Therefore, while in [8] the dilatancy curves rotate in the $\delta : \eta$ plane about a fixed point as M varies, in the present model they are parallel with one another.

Finally, a hardening law for p_s is needed. We will follow tradition, in assuming the classical (non-associative) volumetric hardening law

$$\dot{p}_s = \rho_s p_s \dot{\epsilon}_v^p \tag{5.26}$$

Here

$$\rho_s = \frac{1}{\hat{\lambda} - \hat{\kappa}}, \tag{5.27}$$

where $\hat{\lambda}$ gives the asymptotic slope (i.e., at $\chi_b = 1$) of the isotropic virgin compression curve in the $\epsilon_v : \ln p$ plane.

5.2 Application to Pozzolana Nera

As an example of the capability of the model to reproduce the observed behaviour of real granular materials, we compare theoretical predictions with the experimental results obtained by [10] on Pozzolana Nera, in a series of drained triaxial compression tests at different values of the confining stress.

The values of the material constants adopted in the simulations are summarized in Tab. 1.

The initial values of the state variables assumed for each tests are given in Tab. 2. Note that a single set of internal variables has been used for all the simulations.

Figures 6–7 illustrate the comparison between model predictions and observed behaviour, in the $q : \epsilon_s$ and $\epsilon_v : \epsilon_s$ plane. Overall, a good qualitative and quantitative agreement between predictions and measurements can be observed. In particular, the model appears to reproduce well the transition between a fragile, dilatant behaviour at low confining stresses to a ductile, contractant behaviour at high confining stresses. At high confining stresses, the model is capable to capture the experimentally observed slight reduction in the deviatoric stress at relatively large deviatoric strains, due to the progressive increase of χ_M (i.e., reduction of the slope of the critical state line, M). As for the volumetric behavior, the behavior observed at low confining stress is also captured quite

Table 2: Initial state assumed in the simulations.

test #	p_0 (kPa)	q_0 (kPa)	p_{s0} (kPa)	$\chi_{b,0}$ ($-$)	$\chi_{M,0}$ ($-$)
PN020	214.0	0.0	1800.0	0.556	0.455
PN035	357.0	0.0	1800.0	0.556	0.455
PN140	1404.0	0.0	1800.0	0.556	0.455
PN285	2840.0	0.0	1800.0	0.556	0.455
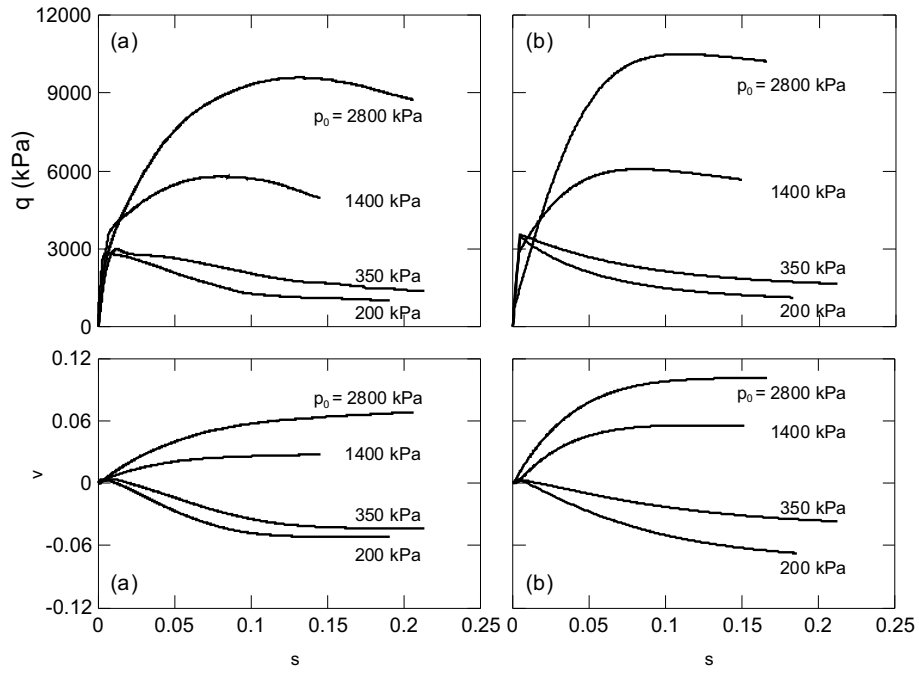
Figure 6: Drained triaxial compression test: a) experimental data; b) model predictions.
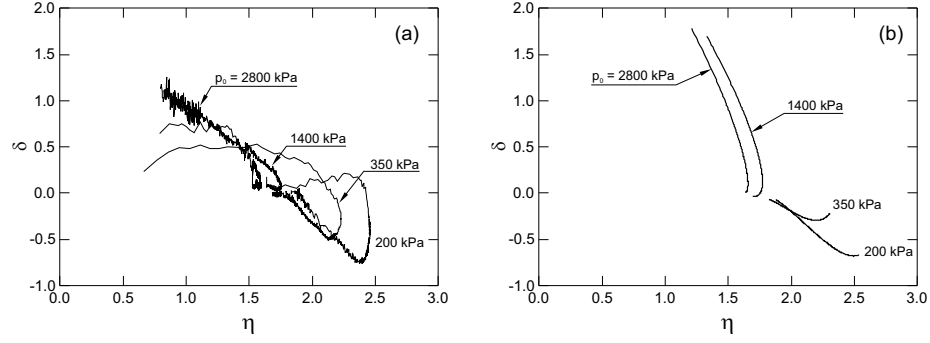
Figure 7: Stress–dilatancy curves: a) experimental data; b) model predictions.

well, whereas computed volumetric strains are sensibly overestimated at small to moderate strains.

The stress–dilatancy curves from the same drained compression tests are plotted in Fig. 7. Here the experimental data on plastic dilatancy are those of [10] and are obtained as follows. It is assumed that axial deformations are entirely plastic, while volumetric plastic deformations are obtained by subtracting from the measured total deformation the elastic component calculated using the experimentally determined swelling coefficient (see [10], equations 2 and 3).

From the figure, it is apparent that the model is capable of reproducing qualitatively, and to a certain extent also quantitatively, the characteristic shape of the experimental curves. In particular, the model correctly predicts that, at all confining stresses, the peak of the stress ratio η always precedes the point of minimum dilatancy δ. The predictions for the two tests at high confining stresses are less satisfactory from a quantitative point of view, due to an overestimation of the dilatancy in the initial part of the test. Even in this case, however, the model captures correctly the shape of the observed stress–dilatancy curves, with the characteristic backward bending before reaching the critical state conditions.

Acknowledgements

References

[1] D. W. Airey. Triaxial testing on naturally cemented carbonate soil. *Journal of Geotechnical Engineering, ASCE*, 119(9):1379–1398, 1993.

[2] R. Al-Douri and H. G. Poulos. Behaviour of pile groups in calcareous sand. *Int. J. Num. Anal. Meth. Geomech.*, 25:49–59, 1994.

[3] S. Aversa and A. Evangelista. The mechanical behaviour of a pyroclastic rock: yield strength and destructuration effects. *Rock Mechanics and Rock Engineering*, 31(1):25–42, 1998.

[4] R. Baker and C. S. Desai. Induced anisotropy during plastic straining. *Int. J. Num. Anal. Meth. Geomech.*, 8:167–185, 1984.

[5] Z. P. Bažant and M. Jirásek. *Inelastic Analysis of Structures*. J. Wiley ans Sons, Chichester, 2002.

[6] D. Bruno, M. F. Randolph, C. W. Cho, and H. A. Joer. Drivability and performance of model piles driven into cemented calcareous sand. In *Stress-wave 2000, VI International Conference on the application of Stress–Wave Theory to Piles*, pages 47–52, Sao Paulo, Brazil, 2000. Balkema, Rotterdam.

[7] R. Castellanza, R. Nova, and C. Tamagnini. Mechanical effects of chemical degradation of bonded geomaterials in boundary value problems. *Revue Francaise de Genie Civil*, 6(Special issue):1169–1192, 2002.

[8] M. Cecconi, A. DeSimone, C. Tamagnini, and G. M. B. Viggiani. A constitutive model for granular materials with grain crushing. *Int. J. Num. Anal. Meth. Geomech.*, 26:1531–1560, 2002.

[9] M. Cecconi and G. M. B. Viggiani. Stability of subvertical cuts in pyroclastic deposits. In *Proc. Geoeng2000*, Melbourne, Australia, 2000.

[10] M. Cecconi and G. M. B. Viggiani. Structural features and mechanical behaviour of a pyroclastic weak rock. *Int. J. Num. Anal. Meth. Geomech.*, 25(15):1525–1557, 2001.

[11] M. Cecconi, G. M. B. Viggiani, A. DeSimone, and C. Tamagnini. A coarse grained weak rock with crushable grains: the Pozzolana Nera from Roma. In C. Viggiani, editor, *Constitutive modelling and analysis of boundary value problems in geotechnical engineering'*, pages 158–185, Napoli, Italy, 2003. Hevelius, Benevento.

[12] I.F. Collins and T. Hilder. A theoretical framework for constructing elastic/plastic constitutive models of triaxial tests. *Int. J. Num. Anal. Meth. Geomech.*, 26:1313–1347, 2002.

[13] I.F. Collins and G. T. Houlsby. Application of thermomechanical principles to the modeling of geotechnical materials. *Proc. Royal Soc. London Series A*, 453:1975–2000, 1997.

[14] M. R. Coop. The influence of particle breakage and state on the behaviour of sands. In *Intl. Workshop on Soil Crushability, IWSC'99*, Yamaguchi, Japan, 2000. Japan Geotechnical Society.

[15] F. Cotecchia and R. J. Chandler. The influence of structure on the prefailure behaviour of a natural clay. *Géotechnique*, 47(3):523–544, 1990.

[16] G. Dyson and M. Randolph. Lateral loading response of piles in calcareous sediments. In *OTRC '99 Conference*, pages 17–36, Austin, TX, 1999. American Society of Civil Engineers.

[17] A. Gens and R. Nova. Conceptual bases for a constitutive model for bonded soils and weak rocks. In Anagnostopoulos et al., editors, *Hard Soils–Soft Rocks*, Athens, Greece, 1993. Balkema, Rotterdam.

[18] P. Germain. *Cours de Méchanique des Milieux Continus*. Masson, Paris, 1973.

[19] P. Germain, Q. S. Nguyen, and P. Suquet. Continuum thermodynamics. *Journal of Applied Mechanics, ASME*, 50:1010–1020, 1983.

[20] M. E. Gurtin. *Thermomechanics of Evolving Phase Boundaries in the Plane*. Clarendon Press, Oxford, 1993.

[21] M. Gutierrez and K. Ishihara. Non–coaxiality and energy dissipation in granular materials. *Soils and Foundations*, 40(2):49–59, 2000.

[22] B. Halphen and Q. S. Nguyen. Sur les matériaux standards généralisés. *Journal de Mécanique*, 14:39–63, 1975.

[23] W. Han and B. D. Reddy. *Plasticity: Mathematical Theory and Numerical Analysis*. Springer Verlag, New York, 1999.

[24] B.O. Hardin. Crushing of soil particles. *Journal of Geotechnical Engineering, ASCE*, 111(10):1177–1192, 1985.

[25] I. Herle and G. Gudehus. Determination of parameters of a hypoplastic constitutive model from properties of grain assemblies. *Mech. Cohesive–Frictional Materials*, 4:461–486, 1999.

[26] G. T. Houlsby. *A study of plasticity theories and their applicability to soils*. PhD thesis, Cambridge University, 1981.

[27] G.T. Houlsby. The use of a variable shear modulus in elastic–plastic models for clays. *Comp. & Geotechnics*, 1:3–13, 1985.

[28] G.T. Houlsby and A.M. Puzrin. A thermomechanical framework for constitutive models for rate–independent dissipative materials. *Int. J. Plasticity*, 16:1017–1047, 2000.

[29] P. V. Lade. Elastoplastic stress–strain theory for cohesionless soil with curved yield surfaces. *Int. Journal of Solids and Structures*, 13(11):1019–1035, 1977.

[30] P.V. Lade, J.A. Yamamuro, and P.A. Bopp. Significance of particle crushing in granular materials. *Journal of Geotechnical Engineering, ASCE*, 122(4):309–316, 1996.

[31] R. Lagioia and R. Nova. An experimental and theoretical study of the behaviour of a calcarenite in triaxial compression. *Géotechnique*, 45(4):633–648, 1995.

[32] R. Lagioia, A. M. Puzrin, and D. M. Potts. A new versatile expression for yield and plastic potential surfaces. *Comp. & Geotechnics*, 19:171–191, 1996.

[33] Maccarini M. *Laboratory studies of a weakly bonded artificial soil.* PhD thesis, Imperial College of science Technology and Medicine, University of London, 1987.

[34] G. A. Maugin. *Thermomechanics of plasticity and fracture.* Cambridge University Press, 1992.

[35] G.R. McDowell and M. Bolton. On the micromechanics of crushable aggregates. *Géotechnique*, 48(5):667–679, 1998.

[36] K. Miura, K. Maeda, and S. Toki. Method of measurement for the angle of repose of sands. *Soils and Foundations*, 37(2):89–96, 1997.

[37] L. Modaressi, L. Laloui, and D. Aubry. Thermodynamical approach for camclay–family models with roscoe–type dilatancy rules. *Int. J. Num. Anal. Meth. Geomech.*, 18:133–138, 1994.

[38] J. J. Moreau. Sur les lois de frottement, de viscosité et de plasticité. *C. R. Acad. Sci.*, 271:608–611, 1970.

[39] Y. Nakata, Y. Kato, M. Hyodo, A.F.L. Hyde, and H. Murata. One dimensional compression behaviour of uniform sand related to single particle crushing strength. *Soils and Foundations*, 41(2):39–51, 2001.

[40] R. Nova. On the hardening of soils. *Archiwum Mechaniki Stosowanej*, 29:445–458, 1977.

[41] R. Nova. Sinfonietta classica: an exercise on classical soil modelling. In Saada and Bianchini, editors, *Constitutive Equations for Granular Non–Cohesive Soils*, Cleveland, 1988. Balkema, Rotterdam.

[42] R. Nova. Mathematical modelling of natural and engineered geomaterials. *Eur. Journal of Mechanics A/Solids*, 11:135–154, 1992. special issue.

[43] R. Nova, R. Castellanza, and C. Tamagnini. A constitutive model for bonded geomaterials subject to mechanical and/or chemical degradation. *Int. J. Num. Anal. Meth. Geomech.*, 27:705–732, 2003.

[44] R. Nova and D. M. Wood. A constitutive model for sand in triaxial compression. *Int. J. Num. Anal. Meth. Geomech.*, 3:255–278, 1979.

[45] B.D. Reddy and J.B. Martin. Internal variable formulations of problems in elastoplasticity: constitutive and algorithmic aspects. *Appl. Mech. Reviews*, 47:429–456, 1993.

[46] T. R. Rockafellar. *Convex Analysis.* Princeton University Press, 1970.

[47] K. H. Roscoe and J. B. Burland. On the generalised stress–strain behaviour of 'wet' clay. In J. Heyman and F. A. Leckie, editors, *Engineering Plasticity*, Cambridge, U.K., 1968.

[48] K. H. Roscoe, A. N. Schofield, and C. P. Wroth. On the yielding of soils. *Géotechnique*, 8:22–53, 1958.

[49] K. H. Roscoe, A. N. Schofield, and C. P. Wroth. On the yielding of soils: Correspondence. *Géotechnique*, 9:71–83, 1959.

[50] M. Rouainia and D. Muir Wood. A kinematic hardening constitutive model for natural clays with loss of structure. *Géotechnique*, 50(2):153–164, 2000.

[51] P. W. Rowe. The stress–dilatancy relation for static equilibrium of an assembly of particles in contact. *Proc. Royal Soc. London*, A269:500–527, 1962.

[52] P. W. Rowe. Theoretical meaning and observed values of deformation parameters for soil. In R. H. G. Parry, editor, *Stress–strain behaviour of soils*, Henley-on-Thames, U.K., 1972.

[53] A. N. Schofield and C. P. Wroth. *Critical State Soil Mechanics*. McGraw Hill, London, 1968.

[54] J. C. Simo. *Numerical Analysis and Simulation of Plasticity*, volume VI of *Handbook of Numerical Analysis*, pages 183–499. Elsevier Science, 1998.

[55] H. A. M. van Eekelen. Isotropic yield surfaces in three dimensions for use in soil mechanics. *Int. J. Num. Anal. Meth. Geomech.*, 4:89–101, 1980.

[56] D. M. Wood. *Soil Behaviour and Critical State Soil Mechanics*. Cambridge University Press, Cambridge, 1990.